

**Reference Correlation for the Thermal Conductivity  
of Ammonia from the Triple-Point Temperature to 680 K and Pressures up to 80 MPa**

**S. A. Monogenidou,<sup>1</sup> M. J. Assael,<sup>1</sup> M. L. Huber<sup>2,a)</sup>**

<sup>1</sup>*Laboratory of Thermophysical Properties and Environmental Processes,*

*Chemical Engineering Department, Aristotle University, Thessaloniki 54636, Greece*

<sup>2</sup>*Applied Chemicals and Materials Division, National Institute of Standards and Technology,*

*325 Broadway, Boulder, CO 80305, USA*

This paper presents a new wide-ranging correlation for the thermal conductivity of ammonia based on critically evaluated experimental data. The correlation is designed to be used with a recently published equation of state that is valid from the triple-point temperature to 680 K and pressures up to 80 MPa. We estimate the uncertainty at a 95% confidence level to be 6.8% over the aforementioned range, with the exception of the dilute-gas range where the uncertainty is 4% over the temperature range 285 K to 575 K. The uncertainties will be larger outside of the validated range, and also in the critical region.

Key words: ammonia; thermal conductivity; transport properties.

---

<sup>a)</sup> Author to whom correspondence should be addressed ([marcia.huber@nist.gov](mailto:marcia.huber@nist.gov))

## CONTENTS

1. Introduction
2. The Correlation
  - 2.1. The dilute-gas limit
  - 2.2. The residual term
  - 2.3. The critical enhancement term
3. Recommended Values
4. Conclusion
5. References

### List of Tables

1. Thermal conductivity measurements of ammonia.
2. Coefficients of Eq. (7) for the residual thermal conductivity of ammonia.
3. Evaluation of the ammonia thermal conductivity correlation for the primary data.
4. Evaluation of the ammonia thermal conductivity correlation for the secondary data.
5. Thermal conductivity values of ammonia along the saturation curve, calculated by the present correlation.
6. Thermal conductivity values of ammonia at selected temperatures and pressures, calculated by the present correlation.

### List of Figures

1. Temperature-pressure range of the primary experimental thermal conductivity data for ammonia.
2. Temperature-density range of the primary experimental thermal conductivity data for ammonia.
3. Dilute-gas limit thermal conductivity of ammonia as a function of temperature.
4. Percentage deviations of the dilute-gas limit thermal conductivity experimental data of ammonia from Eq. (6) as a function of temperature.
5. Percentage deviations of primary thermal conductivity experimental data of ammonia from the values calculated by the present model as a function of temperature.
6. Percentage deviations of primary thermal conductivity experimental data of ammonia from the values calculated by the present model as a function of pressure.

7. Percentage deviations of primary thermal conductivity experimental data of ammonia from the values calculated by the present model as a function of density.
8. Thermal conductivity of ammonia as a function of temperature for selected pressures
9. Thermal conductivity of ammonia as a function of density for selected temperatures

## 1. Introduction

In a series of recent papers, new reference correlations for the thermal conductivity of some simple fluids,<sup>1-4</sup> hydrocarbons,<sup>5-13</sup> alcohols,<sup>14</sup> and refrigerants<sup>15, 16</sup> were reported. In this paper, the methodology adopted in the aforementioned papers is extended to developing a new reference correlation for the thermal conductivity of ammonia.

In 1984, Tufeu *et al.*<sup>17</sup> reported measurements of the thermal conductivity of ammonia, in the temperature range 381–578 K and up to 80 MPa pressure, with an estimated uncertainty of 2%. They further attempted to develop a semiempirical correlation to be employed to calculate the thermal conductivity in the supercritical region. Following this, in 1988, Clifford and Tufeu<sup>18</sup> extended those measurements down to 300 K. Since then, new thermal-conductivity data have been published by Shamsetdinov *et al.*,<sup>19</sup> and a new Helmholtz equation of state of Gao *et al.*<sup>20</sup> has been developed. Furthermore, in a companion paper<sup>21</sup> a new reference correlation for the viscosity of ammonia was proposed. The goal of this work is to critically assess the available literature data and provide a wide-ranging correlation for the thermal conductivity of ammonia that is valid over gas, liquid, and supercritical states, and that incorporates densities provided by the new equation of state of Gao *et al.*<sup>20</sup>

The analysis will be applied to the best available experimental data for the thermal conductivity. Thus, a prerequisite to the analysis is a critical assessment of the experimental data. For this purpose, two categories of experimental data are defined: primary data, employed in the development of the correlation, and secondary data, used simply for comparison purposes. According to the recommendation adopted by the Subcommittee on Transport Properties (now known as The International Association for Transport Properties) of the International Union of Pure and Applied Chemistry, the primary data are identified by a well-established set of criteria.<sup>22</sup> These criteria have been successfully employed to establish standard reference values for the viscosity and thermal conductivity of fluids over wide ranges of conditions, with uncertainties in the range of 1%. However, in many cases, such a narrow definition unacceptably limits the range of the data representation. Consequently, within the primary data set, it is also necessary to include results that extend over a wide range of conditions, albeit with a poorer accuracy, provided they are consistent with other more accurate data or with theory. In all cases, the accuracy claimed for the final recommended data must reflect the estimated uncertainty for the primary information.

## 2. The Correlation

The thermal conductivity  $\lambda$  can be expressed as the sum of three independent contributions, as

$$\lambda(\rho, T) = \lambda_o(T) + \Delta\lambda(\rho, T) + \Delta\lambda_c(\rho, T), \quad (1)$$

where  $\rho$  is the density,  $T$  is the temperature, and the first term,  $\lambda_o(T) = \lambda(0, T)$ , is the contribution to the thermal conductivity in the dilute-gas limit, where only two-body molecular interactions occur. The final term,

$\Delta\lambda_c(\rho, T)$ , the critical enhancement, arises from the long-range density fluctuations that occur in a fluid near its critical point, which contribute to divergence of the thermal conductivity at the critical point. Finally, the term  $\Delta\lambda(\rho, T)$ , the residual property, represents the contribution of all other effects to the thermal conductivity of the fluid at elevated densities.

TABLE 1. Thermal conductivity measurements of ammonia.

1 <sup>st</sup> author	Year Publ.	Technique employed <sup>a</sup>	Purity (%)	Uncertainty (%)	No. of data	Temperature range (K)	Pressure range (MPa)
<b>Primary Data</b>							
Shamsetdinov <sup>19</sup>	2013	HW	99.95	1.5	55	285–354	0.1–20
Clifford <sup>18</sup>	1988	CC	99.96	2.0	20	295–387	0.94–51
Tufeu <sup>17</sup>	1984	CC	99.96	2.0	122	381–578	1–80
Srivastava <sup>23</sup>	1966	HW	na	2.0	9	311–473	0.02
Needham <sup>24</sup>	1965	CC	99.98	2.0	98	293–450	0.1–49
Golubev <sup>25</sup>	1964	HW	na	2.0	133	198–674	0.1–40
Keyes <sup>26</sup>	1954	AHF	na	na	9	323–523	0–0.9
<b>Secondary Data</b>							
Afshar <sup>27</sup>	1981	THW	99.99	4.8-1.5	38	359–924	0.01–0.05
Barua <sup>28</sup>	1968	HW	na	na	3	247–293	0.1
Correia <sup>29</sup>	1968	HW	na	1	6	276–767	0.1
Gutweiler <sup>30</sup>	1968	HW	99.50	2.0	5	339–531	0.1
Baker <sup>31</sup>	1965	THW	na	0.3	4	299–475	0.1
Senftleben <sup>32</sup>	1965	na	na	2	8	273–673	0.1
Richter <sup>33</sup>	1964	CS	na	3.0	38	277–477	0.1–36
Varlaskin <sup>34</sup>	1963	AHF	na	na	5	199–236	0.1
Gray <sup>35</sup>	1961	HW	na	1.0	4	298–422	0.1
Franck <sup>36</sup>	1951	HW	na	1.0	6	394–584	0.02–0.06
Dickins <sup>37</sup>	1934	HW	purified	0.4	1	285	0.01
Kardos <sup>38</sup>	1934	HW	na	na	4	263–293	1.18

<sup>a</sup> AHF, Axial Heat Flow; CC, Concentric Cylinders; CS, Concentric Spheres; HW, Hot Wire; na, not available; THW, Transient Hot Wire;

Table 1 summarizes, to the best of our knowledge, the experimental measurements<sup>17-19,23-38</sup> of the thermal conductivity of ammonia reported in the literature. As already mentioned, in 1984 Tufeu *et al.*<sup>17</sup> reported measurements of the thermal conductivity of ammonia, while in 1988 Clifford and Tufeu<sup>18</sup> extended those measurements down to 300 K. Both these experiments were performed in the same concentric-cylinders instrument with an uncertainty of 2%, and are probably the best measurements today. Hence they are part of our primary data set. However, we note that Clifford and Tufeu<sup>18</sup> stated that the measurements of Tufeu *et*

*al.*<sup>17</sup> performed at 385 K and the highest density point at 412.4 K are considered to be in error, and thus they are not included in the present primary data set.

Four other sets of measurements were investigated by Tufeu *et al.*:<sup>17</sup> those of Srivastava and Das Gupta,<sup>23</sup> Needham and Ziebland,<sup>24</sup> Golubev and Sokolova,<sup>25</sup> and Keyes.<sup>26</sup> The measurements of Srivastava and Das Gupta<sup>23</sup> and Golubev and Sokolova<sup>25</sup> were performed in hot-wire instruments, while the measurements of Needham and Ziebland<sup>24</sup> were performed in a concentric-cylinders instrument. These three sets, obtained with a 2% quoted uncertainty, were also included in our primary data set. It should, however, be pointed out that Tufeu *et al.*<sup>17</sup> observed discrepancies in the critical region between their measurements and those of Golubev and Sokolova<sup>25</sup> and Needham and Ziebland.<sup>24</sup> For this reason, and since we have the very accurate measurements by Tufeu *et al.*<sup>17</sup> in the critical region, it was preferred not to include the near-critical isotherms of Golubev and Sokolova<sup>25</sup> ( $T = 406, 414$  and  $423$  K) and Needham and Ziebland<sup>24</sup> ( $411$  K). Finally, since dissociation of ammonia has been observed above  $700$  K,<sup>21</sup> it was decided not to include the last two measurements of Golubev and Sokolova<sup>25</sup> (at  $T = 723$  and  $773$  K). The measurements of Keyes,<sup>26</sup> performed in an axial heat-flow instrument, were also included in the primary data set, as they are the only other set of gaseous measurements obtained up to  $T = 523$  K.

Since the work of Clifford and Tufeu,<sup>18</sup> Shamsetdinov *et al.*<sup>19</sup> in 2013 measured the thermal conductivity of gaseous and liquid ammonia over a wider range of conditions with a steady-state hot wire and a 1.5% uncertainty. These measurements backed by a full theory, in a well-known instrument, are also included in the primary data set. The remaining measurements were not considered in the primary data set.

Figures 1 and 2 show the ranges of the primary measurements outlined in Table 1, and the phase boundary may be seen as well. The development of the correlation requires densities; Gao *et al.*<sup>20</sup> very recently developed an accurate, wide-ranging equation of state that is valid from the triple point up to  $T = 725$  K and pressures up to 1000 MPa. The equation of state has an uncertainty in density of 0.05% for the vapor phase at temperatures between 200 K and 404 K, an uncertainty of 0.1% for saturated liquid density at temperatures between 195 K and 400 K, and uncertainties in saturated vapor density of 2% for temperatures between 220 K and 395 K. We also adopt the values for the critical point from their equation of state; the critical temperature,  $T_c$ , and the critical density,  $\rho_c$ , are 405.56 K and  $233.250 \text{ kg m}^{-3}$ , respectively.<sup>20</sup> The triple-point temperature employed is 195.49 K.<sup>20</sup> Note that the value of the critical density of  $233.25 \text{ kg m}^{-3}$  proposed by the new correlation of Gao *et al.*<sup>20</sup> is different from the value of  $225.00 \text{ kg m}^{-3}$  employed by the previous Tillner-Roth and Harms-Watzenberg<sup>39</sup> equation of state.

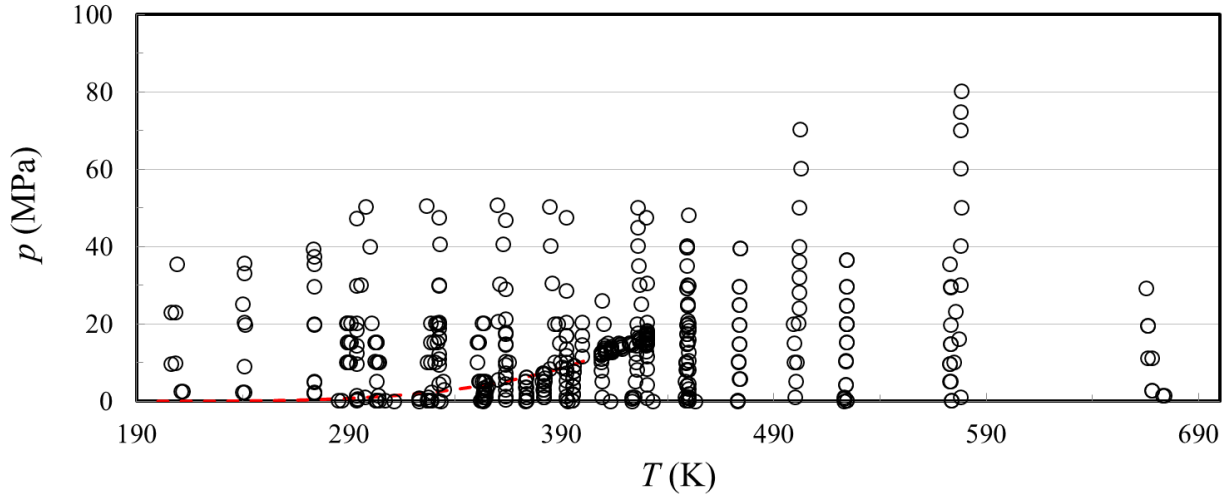


FIG. 1. Temperature-pressure range of the primary experimental thermal conductivity data for ammonia. (—) saturation curve.

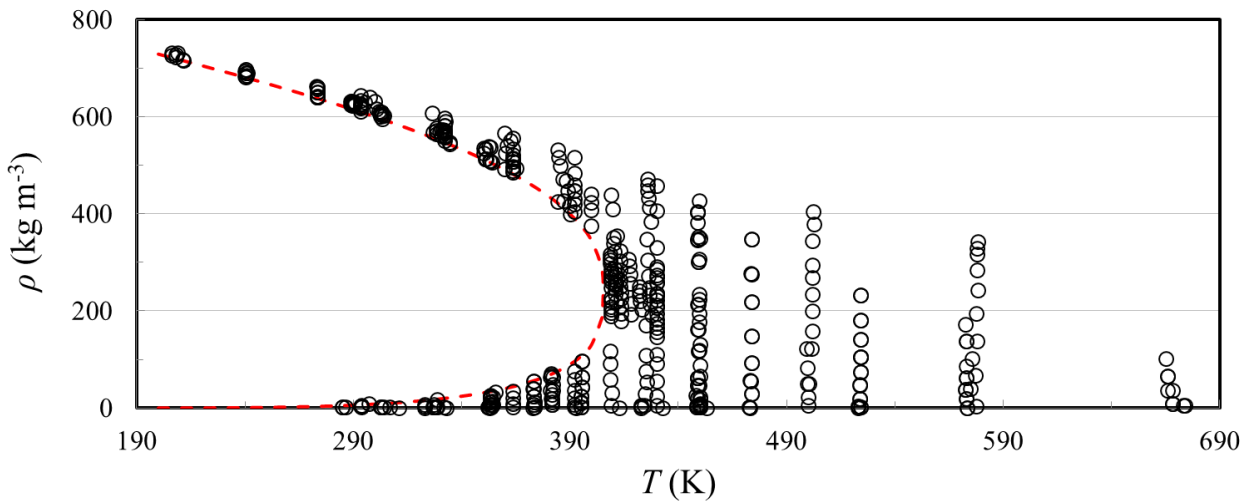


FIG. 2. Temperature-density range of the primary experimental thermal conductivity data for ammonia. (—) saturation curve.

## 2.1. The dilute-gas limit

In order to extrapolate the temperature range of the measurements, a theoretically based scheme was used to correlate the dilute-gas limit thermal conductivity,  $\lambda_o(T)$ , over a wide temperature range. The traditional kinetic approach for thermal conductivity results in an expression involving three generalized cross sections.<sup>40, 41</sup> However, it is possible to derive an equivalent kinetic theory expression for thermal conductivity by making use of the approach of Thijsse *et al.*,<sup>42</sup> and Millat *et al.*,<sup>43</sup> where one considers expansion in terms of total energy, rather than separating translational from internal energy as is done

traditionally. In this case, the dilute-gas limit thermal conductivity,  $\lambda_o(T)$  ( $\text{mW m}^{-1} \text{K}^{-1}$ ), of a polyatomic gas can be shown to be inversely proportional to a single generalized cross section, <sup>40-43</sup>  $S(10E)$  ( $\text{nm}^2$ ), as

$$\lambda_o(T) = 1000 \frac{5k_B^2(1+r^2)T}{2m \langle v \rangle_o S(10E)} f_\lambda, \quad (2)$$

where  $k_B$  is the Boltzmann constant,  $T$  (K) is the absolute temperature,  $f_\lambda$  (-) is the dimensionless higher-order correction factor,  $m$  (kg) is the molecular mass of ammonia, and  $\langle v \rangle_o = 4\sqrt{k_B T / \pi m}$  (m/s) is the average relative thermal speed. The dimensionless quantity  $r^2$  is defined by  $r^2 = 2C_{\text{int}}^o / 5k_B$ , where  $C_{\text{int}}^o$  is the contribution of both the rotational,  $C_{\text{rot}}^o$ , and the vibrational,  $C_{\text{vib}}^o$ , degrees of freedom to the isochoric ideal-gas heat capacity  $C_v^o$ .

The classical trajectory calculations<sup>44-46</sup> confirm that, for most molecules studied, the higher-order thermal-conductivity correction factor is near unity. One can take advantage of this finding to define the effective generalized cross section  $S_\lambda (= S(10E)/f_\lambda)$  ( $\text{nm}^2$ ), and rewrite Eq. (2) for the dilute-gas limit thermal conductivity of ammonia,  $\lambda_o(T)$  ( $\text{mW m}^{-1} \text{K}^{-1}$ ), as

$$\lambda_o(T) = 0.1351767 \frac{(C_p^o / k_B) \sqrt{T}}{S_\lambda}. \quad (3)$$

The ideal-gas isobaric heat capacity per molecule,  $C_p^o (= C_{\text{int}}^o + 2.5k_B)$  in (J/K), can be obtained from Gao *et al.*<sup>20</sup>

$$\frac{C_p^o}{k_B} = c_0 + \sum_{k=1}^3 \nu_k \left( \frac{u_k}{T} \right)^2 \frac{\exp(u_k / T)}{[\exp(u_k / T) - 1]^2}, \quad (4)$$

where the values of the coefficients of Eq. (4) are  $c_0 = 4$ ,  $\nu_1 = 2.224$ ,  $\nu_2 = 3.148$ ,  $\nu_3 = 0.9579$ ,  $u_1 = 1646$ ,  $u_2 = 3965$ , and  $u_3 = 7231$ . It has been previously noted, and recently confirmed<sup>41</sup> for smaller molecules, that the cross section  $S(10E)$  exhibits a nearly quadratic dependence on the inverse temperature. Hence, in order to develop the correlation, we have employed dilute-gas thermal-conductivity measurements to fit the effective cross section  $S_\lambda$  ( $\text{nm}^2$ ), by means of Eqs. (3) and (4), as a function of the inverse temperature. For this task we employed the dilute-gas thermal-conductivity measurements of Tufeu *et al.*,<sup>17</sup> as well as the dilute-gas measurements of Needham and Ziebland,<sup>24</sup> Keyes,<sup>26</sup> and Srivastava and Das Gupta,<sup>23</sup> and the more recent measurements of Shamsetdinov *et al.*<sup>19</sup> The equation obtained is

$$S_\lambda = 0.07152 + \frac{130.228}{T} - \frac{9569.817}{T^2}. \quad (5)$$

Equations (3) – (5) form a consistent set of equations for the calculation of the dilute-gas limit thermal conductivity of ammonia.



The values of the dilute-gas limit thermal conductivity,  $\lambda_0(T)$  in  $\text{mW m}^{-1} \text{K}^{-1}$ , obtained by the scheme of Eqs. (3) – (5), were fitted as a function of the reduced temperature  $T_r = T/T_c$  for ease of use to the following equation:

$$\lambda_0(T) = \frac{86.9294 - 170.5502 T_r + 608.0287 T_r^2 - 100.9764 T_r^3 + 85.1986 T_r^4}{4.68994 + 9.21307 T_r - 1.53637 T_r^2 + T_r^3}. \quad (6)$$

Values calculated by Eq. (6) do not deviate from the values calculated by the scheme of Eqs. (3)–(5) by more than 0.07% over the temperature range from 285 K to 575 K. Equation (6) is hence employed in the calculations that will follow.

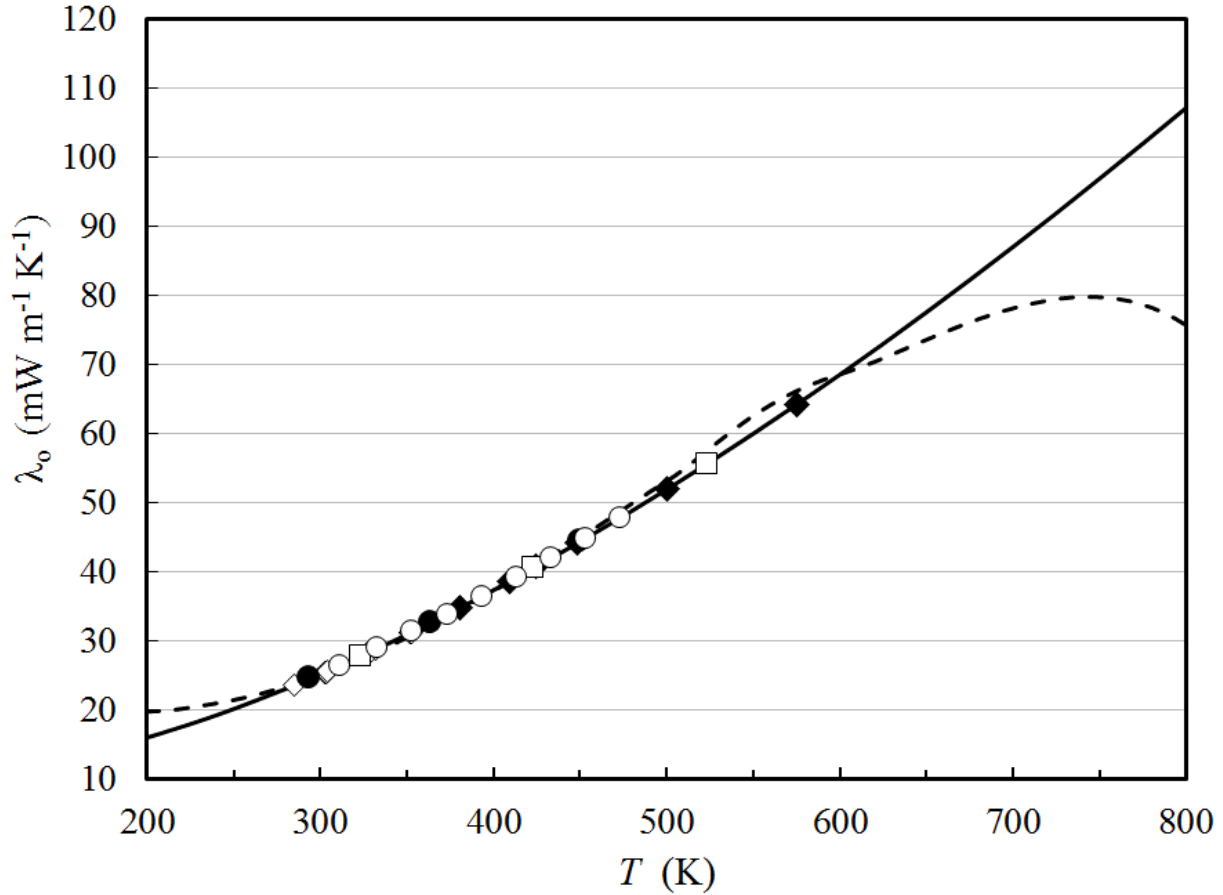


FIG. 3. Dilute-gas limit thermal conductivity of ammonia as a function of temperature. Tufeu *et al.*<sup>17</sup> ( $\blacklozenge$ ), Shamsetdinov *et al.*<sup>19</sup> ( $\diamond$ ), Srivastava and Das Gupta<sup>23</sup> ( $\circ$ ), Needham and Ziebland<sup>24</sup> ( $\bullet$ ), Keyes<sup>26</sup> ( $\square$ ), correlation of Tufeu *et al.* (- -) (valid between 300-580 K), and Eq. (6) (—).

Figure 3 shows the dilute-gas limit thermal conductivity of the selected investigators, and the values calculated by Eq. (6), as a function of the temperature. In Fig. 4, percentage deviations of the dilute-gas limit

thermal conductivity of ammonia from Eq. (6) are shown. The 1984 Tufeu *et al.*<sup>17</sup> dilute-gas thermal-conductivity correlation is also shown in both figures. Considering that Tufeu's correlation is a fourth-order polynomial, valid between 300 to 580 K with a standard uncertainty of 2% (i.e. 4% at the 95% confidence level), the agreement is excellent. Furthermore, since the present correlation has a theoretical background it can safely be extrapolated from the triple point up to 700 K, a temperature at which dissociation of ammonia has been observed.<sup>47</sup>

Based on these measurements, the uncertainty (standard deviation) of the correlation at the 95% confidence level over the temperature range 285 K to 575 K, is 4%. The correlation behaves in a physically reasonable manner over the entire range from the triple point to the highest temperature of the experimental data, 575 K; however, we anticipate the uncertainty may be larger in the areas where data are unavailable and the correlation is extrapolated up to 700 K.

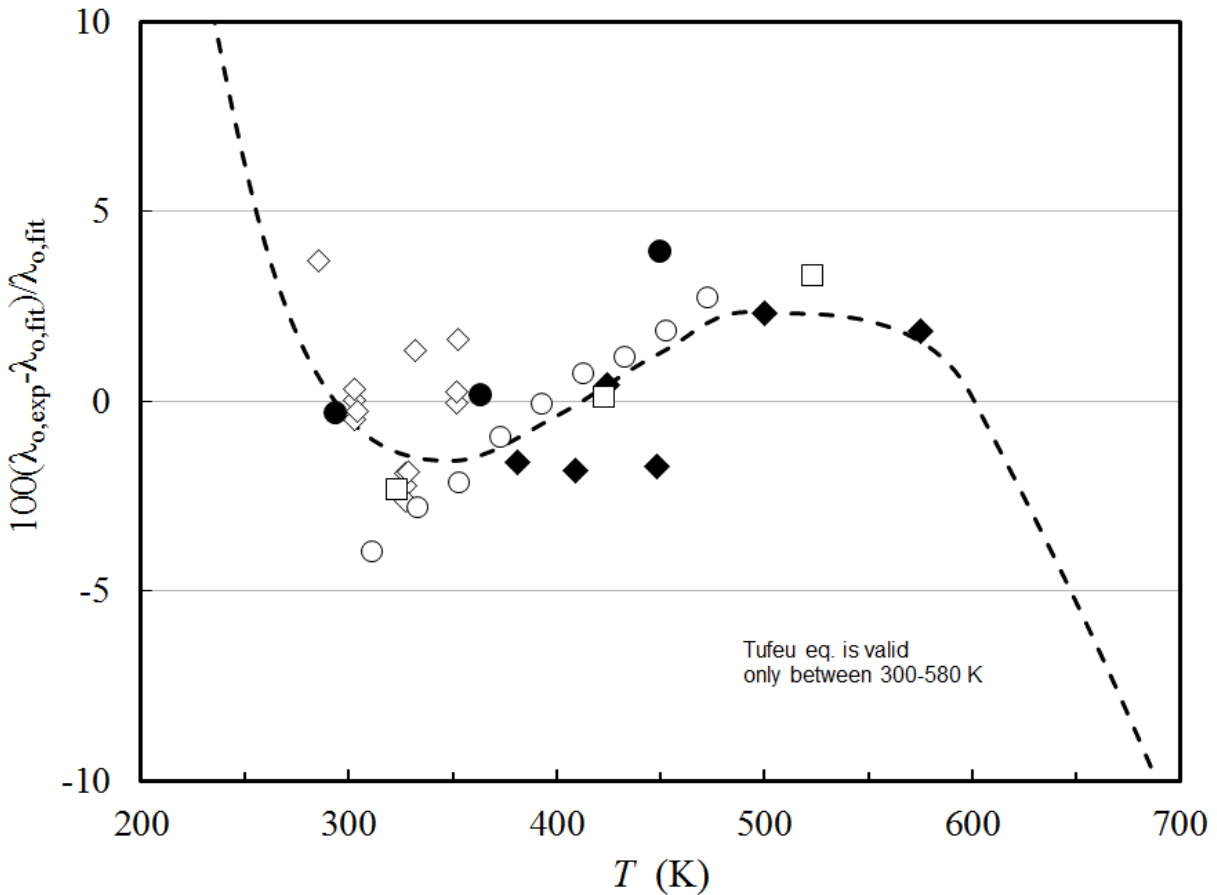


FIG. 4. Percentage deviations of the dilute-gas limit thermal-conductivity measurements of ammonia from Eq. (6) as a function of temperature. Tufeu *et al.*<sup>17</sup> (◆), Shamsetdinov *et al.*<sup>19</sup> (◇), Srivastava and Das Gupta<sup>23</sup> (○), Needham and Ziebland<sup>24</sup> (●), Keyes<sup>26</sup> (□), correlation of Tufeu *et al.* (- -) (valid between 300-580 K).

## 2.2. The residual term

The thermal conductivities of pure fluids exhibit an enhancement over a large range of densities and temperatures around the critical point and become infinite at the critical point. This behavior can be described by models that produce a smooth crossover from the singular behavior of the thermal conductivity asymptotically close to the critical point to the residual values far away from the critical point.<sup>48, 49</sup> The density-dependent terms for thermal conductivity can be grouped according to Eq. (1) as  $[\Delta\lambda(\rho, T) + \Delta\lambda_c(\rho, T)]$ . To assess the critical enhancement theoretically, we need to evaluate, in addition to the dilute-gas thermal conductivity, the residual thermal-conductivity contribution. The procedure adopted in this analysis used ODRPACK<sup>50</sup> to fit all the primary data simultaneously to the residual thermal conductivity and the critical enhancement, while maintaining the values of the dilute-gas thermal-conductivity data already obtained. The density values employed were obtained by the equation of state of Gao *et al.*<sup>20</sup> The primary data were weighted in inverse proportion to the square of their uncertainty.

The residual thermal conductivity was represented with a polynomial in temperature and density:

$$\Delta\lambda(\rho, T) = \sum_{i=1}^5 (B_{1,i} + B_{2,i}(T/T_c)) (\rho/\rho_c)^i. \quad (7)$$

Coefficients  $B_{1,i}$  and  $B_{2,i}$  are shown in Table 2.

TABLE 2. Coefficients of Eq. (7) for the residual thermal conductivity of ammonia.

$i$	$B_{1,i}$ (mW m <sup>-1</sup> K <sup>-1</sup> )	$B_{2,i}$ (mW m <sup>-1</sup> K <sup>-1</sup> )
1	$0.103\ 432 \times 10^0$	$-0.283\ 976 \times 10^{-1}$
2	$-0.112\ 597 \times 10^0$	$0.482\ 520 \times 10^{-1}$
3	$0.233\ 301 \times 10^0$	$-0.644\ 124 \times 10^{-1}$
4	$-0.112\ 536 \times 10^0$	$0.529\ 376 \times 10^{-2}$
5	$0.141\ 129 \times 10^{-1}$	$0.891\ 203 \times 10^{-2}$

## 2.3. The critical enhancement term

The theoretically based crossover model proposed by Olchowy and Sengers<sup>48, 49</sup> is complex and requires solution of a quartic system of equations in terms of complex variables. A simplified crossover model has also been proposed by Olchowy and Sengers.<sup>51</sup> The critical enhancement of the thermal conductivity from this simplified model is given by

$$\Delta\lambda_c = \frac{\rho C_p R_D k_B T}{6\pi \bar{\eta} \xi} (\bar{\Omega} - \bar{\Omega}_0), \quad (8)$$

with

$$\bar{\Omega} = \frac{2}{\pi} \left[ \left( \frac{C_p - C_v}{C_p} \right) \arctan(\bar{q}_D \xi) + \frac{C_v}{C_p} \bar{q}_D \xi \right] \quad (9)$$

and

$$\bar{\Omega}_0 = \frac{2}{\pi} \left[ 1 - \exp \left( - \frac{1}{(\bar{q}_D \xi)^{-1} + (\bar{q}_D \xi \rho_c / \rho)^2 / 3} \right) \right]. \quad (10)$$

In Eqs. (8) – (10),  $\bar{\eta}$  (Pa s) is the viscosity, and  $C_p$  and  $C_v$  (J kg<sup>-1</sup> K<sup>-1</sup>) are the isobaric and isochoric specific heat obtained from the equation of state. The correlation length  $\xi$  (m) is given by

$$\xi = \xi_0 \left( \frac{p_c \rho}{\Gamma \rho_c^2} \right)^{\nu/\gamma} \left[ \left. \frac{\partial \rho(T, \rho)}{\partial p} \right|_T - \left( \frac{T_{\text{ref}}}{T} \right) \left. \frac{\partial \rho(T_{\text{ref}}, \rho)}{\partial p} \right|_T \right]^{\nu/\gamma}. \quad (11)$$

As already mentioned, the coefficients  $B_{1,i}$  and  $B_{2,i}$  in Eq. (7) were fitted with ODRPACK<sup>50</sup> to the primary data for the thermal conductivity of ammonia. This crossover model requires the universal amplitude,  $R_D = 1.02$  (-), and the universal critical exponents,  $\nu = 0.63$  and  $\gamma = 1.239$ , and the system-dependent amplitudes  $\Gamma$  and  $\xi_0$ . For this work, we adopted the values  $\Gamma = 0.053$  (-) and  $\xi_0 = 0.140 \times 10^{-9}$  m, using the universal representation of the critical enhancement of the thermal conductivity by Perkins *et al.*<sup>52</sup> When there are sufficient experimental data available in the critical region, the remaining parameter  $\bar{q}_D^{-1}$  may be found by regression. The data set of Tufeu *et al.*<sup>17</sup> contains data in the critical region, which were used to fit the effective cutoff wavelength  $\bar{q}_D^{-1}$  (m) simultaneously with the coefficients of Eq. (7) and to obtain the value for  $\bar{q}_D^{-1}$  of  $4.0 \times 10^{-10}$  m. The viscosity required for Eq. (8) was obtained by the recent correlation of Monogenidou *et al.*<sup>21</sup> The reference temperature  $T_{\text{ref}}$ , far above the critical temperature where the critical enhancement is negligible, was calculated by  $T_{\text{ref}} = (3/2) T_c$ ,<sup>31</sup> which for ammonia is 608.34 K.

Table 3 summarizes comparisons of the primary data with the correlation. The average absolute percent deviation of the fit is 2.67%, and its bias is -0.18%. We estimate the uncertainty (standard deviation) in thermal conductivity at a 95% confidence level to be 6.8% for the temperature range 200 K to 680 K at pressures up to 80 MPa.

TABLE 3. Evaluation of the ammonia thermal conductivity correlation for the primary data.

1 <sup>st</sup> Author	Year Publ.	AAD (%)	BIAS (%)	MAX (%)
Shamsetdinov <sup>19</sup>	2013	1.83	0.19	5.9
Clifford <sup>18</sup>	1988	2.26	0.09	6.9
Tufeu <sup>17</sup>	1984	1.74	-0.63	9.8
Srivastava <sup>23</sup>	1966	1.90	-0.58	-4.3
Needham <sup>24</sup>	1965	2.80	2.31	13.2
Golubev <sup>25</sup>	1964	3.98	-1.87	12.3
Keyes <sup>26</sup>	1954	2.08	0.50	4.0
<b>Entire data set</b>		<b>2.67</b>	<b>-0.18</b>	

TABLE 4. Evaluation of the ammonia thermal conductivity correlation for the secondary data.

1 <sup>st</sup> Author	Year Publ.	AAD (%)	BIAS (%)	MAX (%)
Afshar <sup>27</sup>	1981	4.57	-4.57	-9.4
Barua <sup>28</sup>	1968	6.61	-6.61	-8.0
Correia <sup>29</sup>	1968	2.01	-1.62	-4.9
Gutweiler <sup>30</sup>	1968	2.95	2.59	4.8
Baker <sup>31</sup>	1965	1.39	-1.39	-2.0
Senftleben <sup>32</sup>	1965	7.65	6.13	20.0
Richter <sup>33</sup>	1964	2.92	-0.52	9.3
Varlaskin <sup>34</sup>	1963	21.61	-21.61	-32.4
Gray <sup>35</sup>	1961	6.84	-6.84	-9.2
Franck <sup>36</sup>	1951	3.93	-3.93	-9.1
Dickins <sup>37</sup>	1934	1.96	-1.96	-2.0
Kardos <sup>38</sup>	1934	15.61	-15.61	-20.4

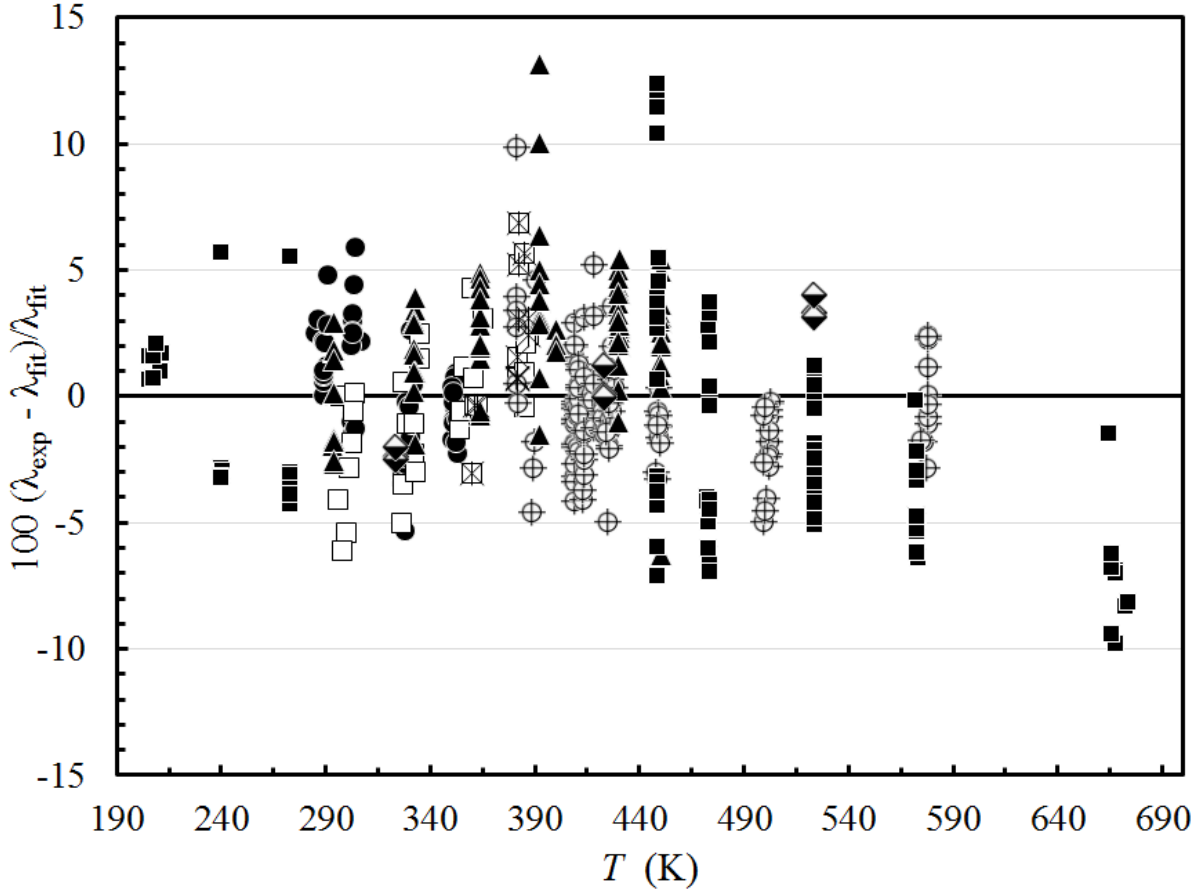


FIG. 5. Percentage deviations of primary thermal conductivity experimental data of ammonia from the values calculated by the present model as a function of temperature. Tufeu *et al.*<sup>17</sup> (⊕), Clifford and Tufeu<sup>18</sup> (□), Shamsedinov *et al.*<sup>19</sup> (●), Srivastava and Das Gupta<sup>23</sup> (△), Needham and Ziebland<sup>24</sup> (▲), Golubev and Sokolova<sup>25</sup> (■), Keyes<sup>26</sup> (◇).

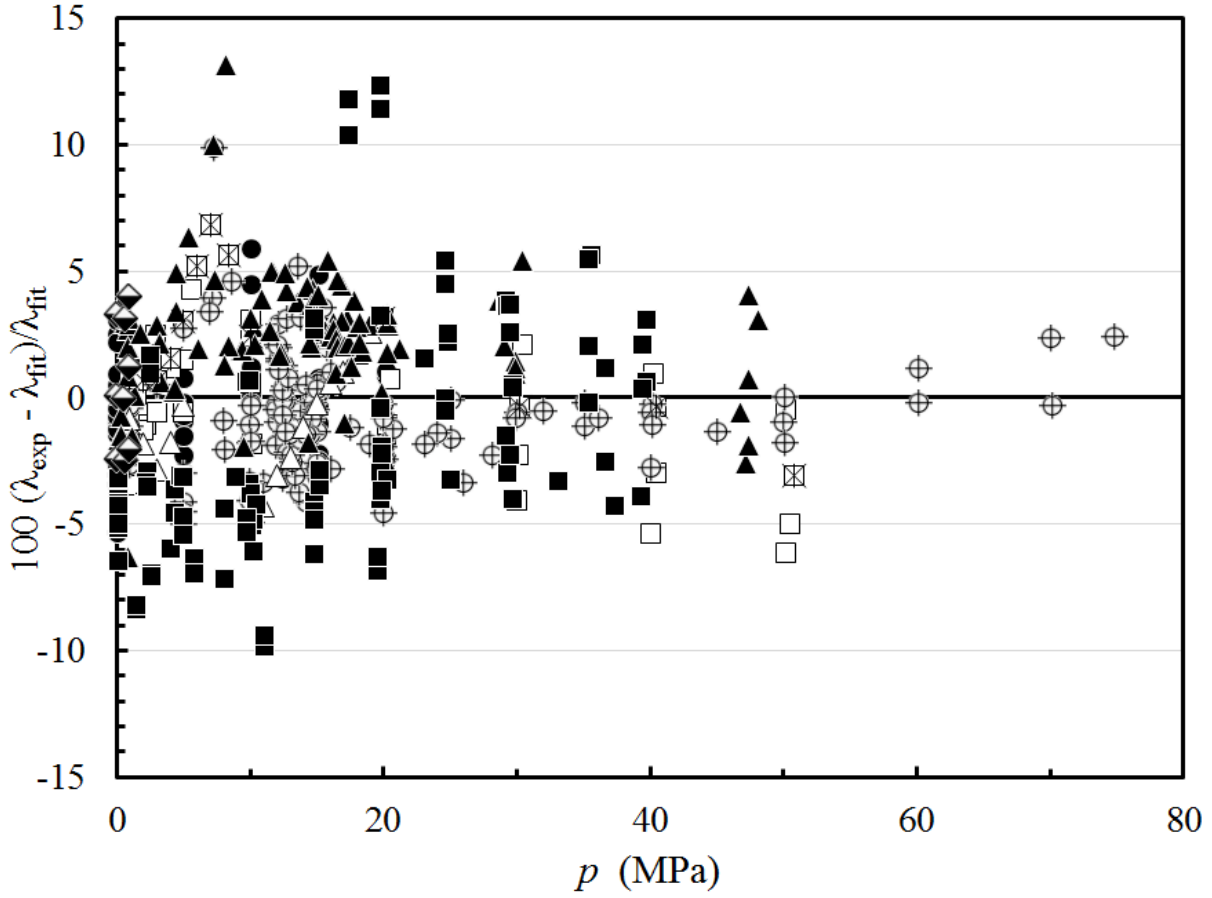


FIG. 6. Percentage deviations of primary thermal conductivity experimental data of ammonia from the values calculated by the present model as a function of pressure. Tufeu *et al.*<sup>17</sup> ( $\oplus$ ), Clifford and Tufeu<sup>18</sup> ( $\square$ ), Shamsetdinov *et al.*<sup>19</sup> ( $\bullet$ ), Srivastava and Das Gupta<sup>23</sup> ( $\triangle$ ), Needham and Ziebland<sup>24</sup> ( $\blacktriangle$ ), Golubev and Sokolova<sup>25</sup> ( $\blacksquare$ ), Keyes<sup>26</sup> ( $\blacklozenge$ ).

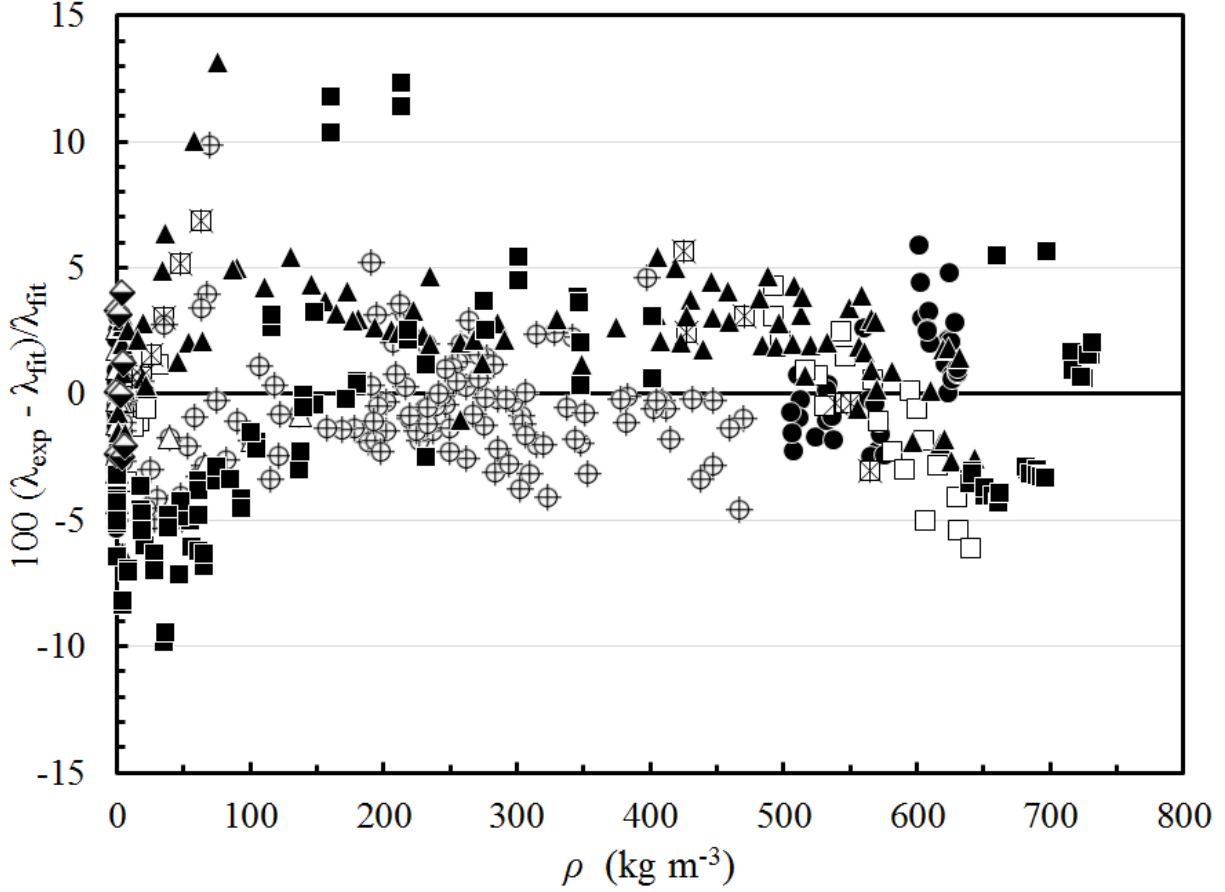


FIG. 7. Percentage deviations of primary thermal conductivity experimental data of ammonia from the values calculated by the present model as a function of density. Tufeu *et al.*<sup>17</sup> ( $\oplus$ ), Clifford and Tufeu<sup>18</sup> ( $\square$ ), Shamsetdinov *et al.*<sup>19</sup> ( $\bullet$ ), Srivastava and Das Gupta<sup>23</sup> ( $\triangle$ ), Needham and Ziebland<sup>24</sup> ( $\blacktriangle$ ), Golubev and Sokolova<sup>25</sup> ( $\blacksquare$ ), Keyes<sup>26</sup> ( $\blacklozenge$ ).

Figure 5 shows the percentage deviations of all primary thermal conductivity data from the values calculated by Eqs. (1) and (6)–(11) as a function of temperature, while Figs. 6 and 7 show the same deviations but as a function of the pressure and the density. Although the experimental data cover a fairly wide range of temperature and pressure, as indicated in Fig. 1, there are few cases where the exact same range of conditions has been measured by more than one investigator. For example, in the liquid phase Shamsetdinov *et al.*<sup>19</sup> measured an isotherm at approximately 290 K over 10.1–20.3 MPa, while Needham and Ziebland<sup>24</sup> measured at 293 K from 1.4 MPa to 29.9 MPa. Both sets of measurements are in agreement with the model to within 4%. Shamsetdinov *et al.*<sup>19</sup> also measured an isotherm at approximately 330 K from 0.1 MPa to 20.3 MPa, while Needham and Ziebland<sup>24</sup> measured at 332.5 K from 4.5 MPa to 29.9 MPa. Clifford and Tufeu<sup>18</sup> measured a total of 4 points at 332.4 K to 334.7 K at pressures from 2.9 MPa to 40.5 MPa. These



measurements all are in agreement with the model to within 4%. In the supercritical region, at approximately 450 K, three investigators<sup>17,24,25</sup> performed measurements that cover 0.1 MPa to 48 MPa. The measurements of Needham and Ziebland<sup>24</sup> generally are in agreement with Tufeu *et al.*<sup>17</sup> to within about 4%, with Golubev and Sokolova<sup>25</sup> exhibiting larger deviations, as seen in Figure 5.

Table 4 shows the average absolute percent deviation (AAD), bias, and maximum percent deviation for the secondary data. Figure 8 shows a plot of the thermal conductivity of ammonia as a function of the temperature for different pressures. The plot demonstrates the smooth extrapolation behavior at conditions outside of the range of experimental data (above 680 K and 80 MPa). The equation of state of Gao *et al.*<sup>20</sup> is valid up to 1000 MPa, but we recommend limiting the use of the present correlation to 100 MPa. Finally, Fig. 9 shows the thermal conductivity of ammonia as a function of the density for different temperatures, including the critical enhancement.

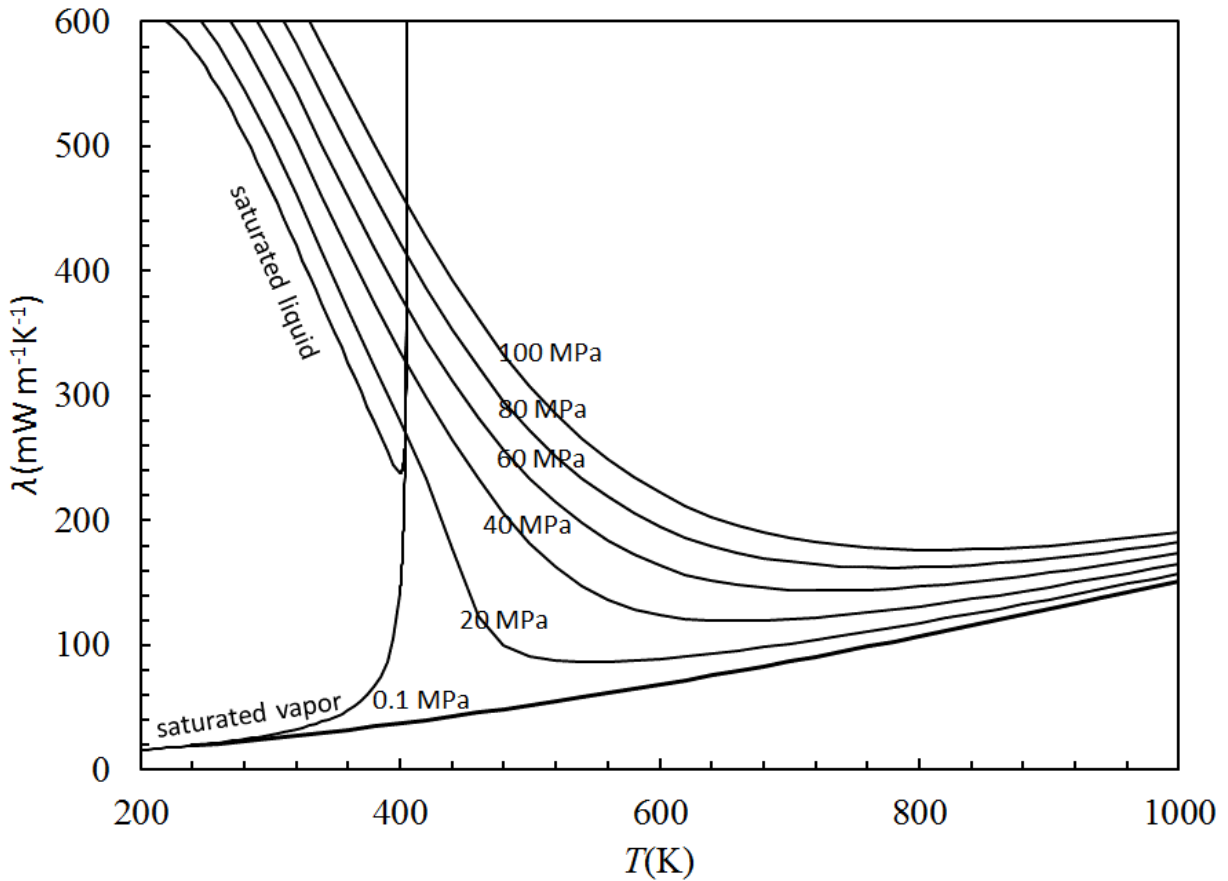


FIG. 8. Thermal conductivity of ammonia as a function of temperature for selected pressures.

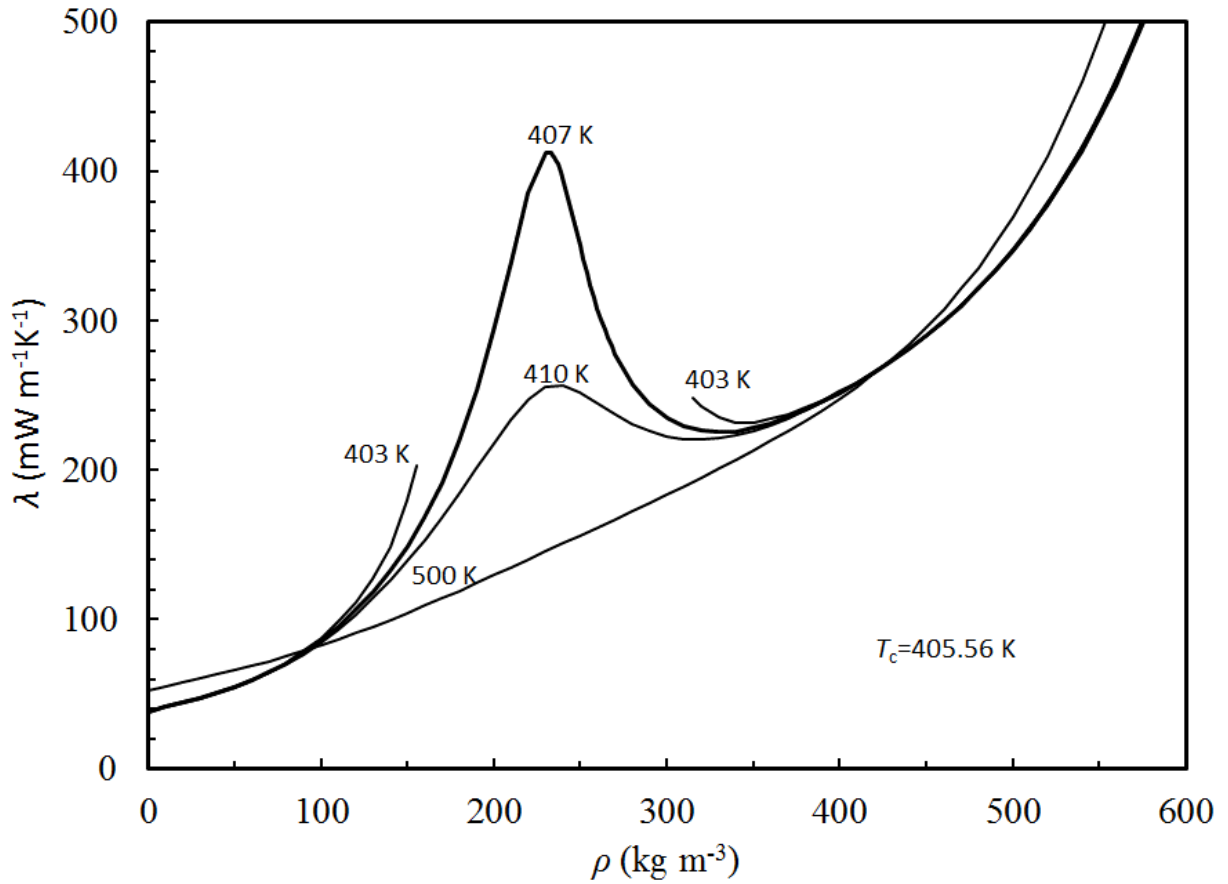


FIG. 9. Thermal conductivity of ammonia as a function of density for selected temperatures.

### 3. Recommended Values

In Table 5, thermal conductivity values are given along the saturation boundary for liquid and vapor, calculated from the present proposed correlations between  $T = 200$  and  $600$  K, while in Table 6 thermal conductivity values are given for temperatures between  $200$  and  $600$  K at selected pressures. Saturation pressure and saturation density values for selected temperatures, as well as the density values for the selected temperature and pressure, are obtained from the equation of state of Gao *et al.*<sup>20</sup> For checking of computer calculations, for  $T = 390$  K, at  $\rho = 415.0$  kg m<sup>-3</sup>, the dilute-gas contribution from Eq. (6) is  $35.969501$  mW m<sup>-1</sup> K<sup>-1</sup>, the residual contribution from Eq. (7) is  $218.750277$  mW m<sup>-1</sup> K<sup>-1</sup>, and the contribution from the critical enhancement in Eqs. (8) - (11) is  $9.409965$  mW m<sup>-1</sup> K<sup>-1</sup>, leading to a value for the thermal conductivity of  $264.129743$  mW m<sup>-1</sup> K<sup>-1</sup>.

TABLE 5. Thermal conductivity values of ammonia along the saturation curve, calculated by the present correlation.

$T$ (K)	$p$ (MPa)	$\rho_{\text{liq}}$ (kg m <sup>-3</sup> )	$\rho_{\text{vap}}$ (kg m <sup>-3</sup> )	$\lambda_{\text{liq}}$ (mW m <sup>-1</sup> K <sup>-1</sup> )	$\lambda_{\text{vap}}$ (mW m <sup>-1</sup> K <sup>-1</sup> )
200	0.0086098	728.67	0.088673	610.35	16.028
225	0.045452	699.55	0.42076	595.66	18.086
250	0.16489	668.97	1.4038	563.72	20.632
275	0.45975	636.11	3.6887	518.92	23.870
300	1.0611	600.17	8.2443	465.89	28.116
325	2.1324	559.80	16.567	408.61	33.938
350	3.8652	512.42	31.336	350.12	42.760
375	6.4853	451.52	58.892	291.57	60.174
400	10.297	344.01	130.89	238.10	142.34

TABLE 6. Thermal conductivity values of ammonia at selected temperatures and pressures, calculated by the present correlation.

$p$ (MPa)	$T$ (K)	$\rho$ (kg m <sup>-3</sup> )	$\lambda$ (mW m <sup>-1</sup> K <sup>-1</sup> )
0.1	200	728.70	610.47
	300	0.68976	25.369
	400	0.51384	37.467
	500	0.41028	51.987
	600	0.34164	68.601
25	200	737.51	643.79
	300	620.59	514.89
	400	456.48	295.99
	500	169.57	114.01
	600	102.47	96.121
50	200	745.67	677.40
	300	637.43	563.26
	400	509.08	358.57
	500	347.35	211.24
	600	221.15	144.69

## 4. Conclusions

A new wide-ranging correlation for the thermal conductivity of ammonia was developed based on critically evaluated experimental data. The correlation is expressed in terms of temperature and density and is designed to be used with the equation of state of Gao *et al.*<sup>20</sup> The estimated uncertainty at a 95% confidence level is estimated to be 6.8% from the triple-point temperature to 680 K and pressures up to 80 MPa, with the exception of the dilute-gas range where the uncertainty is 4% over the temperature range 285 K to 575 K. The correlation may be used in an extrapolation mode up to 100 MPa, but the uncertainties will be larger outside of the validated range, and also in the critical region. In addition, the correlation does not consider dissociation and should not be extrapolated to temperatures above 700 K.

## 5. References

1. M. J. Assael, J. A. M. Assael, M. L. Huber, R. A. Perkins, and Y. Takata, *J. Phys. Chem. Ref. Data* **40**, 033101 (2011).
2. M. J. Assael, I. A. Koini, K. D. Antoniadis, M. L. Huber, I. M. Abdulagatov, and R. A. Perkins, *J. Phys. Chem. Ref. Data* **41**, 023104 (2012).
3. M. L. Huber, R. A. Perkins, D. G. Friend, J. V. Sengers, M. J. Assael, I. N. Metaxa, K. Miyagawa, R. Hellmann, and E. Vogel, *J. Phys. Chem. Ref. Data* **41**, 033102 (2012).
4. M. L. Huber, E. A. Sykioti, M. J. Assael, and R. A. Perkins, *J. Phys. Chem. Ref. Data* **45**, 013102 (2016).
5. M. J. Assael, S. K. Mylona, M. L. Huber, and R. A. Perkins, *J. Phys. Chem. Ref. Data* **41**, 023101 (2012).
6. M. J. Assael, E. K. Michailidou, M. L. Huber, and R. A. Perkins, *J. Phys. Chem. Ref. Data* **41**, 043102 (2012).
7. C.-M. Vassiliou, M. J. Assael, M. L. Huber, and R. A. Perkins, *J. Phys. Chem. Ref. Data* **44**, 033102 (2015).
8. M. J. Assael, I. Bogdanou, S. K. Mylona, M. L. Huber, R. A. Perkins, and V. Vesovic, *J. Phys. Chem. Ref. Data* **42**, 023101 (2013).
9. S. A. Monogenidou, M. J. Assael, and M. L. Huber, *J. Phys. Chem. Ref. Data* **47**, 013103 (2018).
10. A. Koutian, M. J. Assael, M. L. Huber, and R. A. Perkins, *J. Phys. Chem. Ref. Data* **46**, 013102 (2016).
11. M. J. Assael, A. Koutian, M. L. Huber, and R. A. Perkins, *J. Phys. Chem. Ref. Data* **45**, 033104 (2016).
12. S. K. Mylona, K. D. Antoniadis, M. J. Assael, M. L. Huber, and R. A. Perkins, *J. Phys. Chem. Ref. Data* **43**, 043104 (2014).
13. M. J. Assael, T. B. Papalas, and M. L. Huber, *J. Phys. Chem. Ref. Data* **46**, 033103 (2017).
14. E. A. Sykioti, M. J. Assael, M. L. Huber, and R. A. Perkins, *J. Phys. Chem. Ref. Data* **42**, 043101 (2013).
15. R. A. Perkins, M. L. Huber, and M. J. Assael, *J. Chem. Eng. Data* **61**, 3286 (2016).
16. C. M. Tsolakidou, M. J. Assael, M. L. Huber, and R. A. Perkins, *J. Phys. Chem. Ref. Data* **42**, 023103 (2017).

17. R. Tufeu, D. Y. Ivanov, Y. Garrabos, and B. Le Neindre, *Ber. Bunsenges. Phys. Chem.* **88**, 422 (1984).
18. A. A. Clifford and R. Tufeu, *Trans. ASME* **110**, 992 (1988).
19. F. N. Shamsetdinov, Z. I. Zaripov, I. M. Abdulagatov, M. L. Huber, F. M. Gumerov, F. R. Gabitov, and A. F. Kazakov, *Int. J. Refrig.* **36**, 1347 (2013).
20. K. Gao, J. Wu, I. H. Bell, and E. W. Lemmon, (to be submitted, 2018).
21. S. A. Monogenidou, M. J. Assael, and M. L. Huber, *J. Phys. Chem. Ref. Data* **47**, 023102 (2018).
22. M. J. Assael, M. L. V. Ramires, C. A. Nieto de Castro, and W. A. Wakeham, *J. Phys. Chem. Ref. Data* **19**, 113 (1990).
23. B. N. Srivastava and A. Das Gupta, *Phys. Fluids* **9**, 722 (1966).
24. D. P. Needham and H. Ziebland, *Int. J. Heat Mass Transfer* **8**, 1387 (1965).
25. I. F. Golubev and V. P. Sokolova, *Thermal Eng.* **11**, 78 (1964).
26. F. G. Keyes, *Trans. ASME* **76**, 809 (1954).
27. R. Afshar, S. Murad, and S. C. Saxena, *Chem. Eng. Comm.* **10**, 1 (1981).
28. A. K. Barua, A. Manna, and P. Mukhopadhyay, *J. Chem. Phys.* **49**, 2422 (1968).
29. P. Correia, B. Schramm, and K. Schafer, *Ber. Bunsen-Ges.* **72**, 393 (1968).
30. J. Gutweiler and C. J. G. Raw, *J. Chem. Phys.* **48**, 2413 (1968).
31. C. E. Baker and R. S. Brokaw, *J. Chem. Phys.* **43**, 3519 (1965).
32. V. H. Senftleben, *Z. Phys.* **17**, 86 (1964).
33. N. G. Richter and B. H. Sage, *J. Chem. Eng. Data* **9**, 75 (1964).
34. P. G. Varlaskin and J. C. Thompson, *J. Chem. Eng. Data* **8**, 526 (1963).
35. P. Gray and P. G. Wright, *Proc. R. Soc. London, Ser. A* **263**, 161 (1961).
36. E. U. Franck, *Z. Elektrochem.* **55**, 636 (1951).
37. B. G. Dickins, *Proc. R. Soc. London, Ser. A* **143**, 517 (1934).
38. A. Kardos, *Z. Gesamte Kalte-Ind.* **41**, 29 (1934).
39. R. Tillner-Roth and F. Harms-Watzenberg, *DKV Tagungsbericht* **20**, 167 (1993).
40. R. Hellmann, E. Bich, E. Vogel, and V. Vesovic, *J. Chem. Eng. Data* **57**, 1312 (2012).
41. F. R. W. McCourt, J. J. M. Beenakker, W. E. Köhler, and I. Kučšer, *Nonequilibrium Phenomena in Polyatomic Gases* (Clarendon Press, Oxford, 1990).
42. B. J. Thijssen, G. W. Thooft, D. A. Coombe, H. F. P. Knaap, and J. J. M. Beenakker, *Physica A* **98**, 307 (1979).
43. J. Millat, V. Vesovic, and W. A. Wakeham, *Physica A* **148**, 153 (1988).
44. S. Bock, E. Bich, E. Vogel, A. S. Dickinson, and V. Vesovic, *J. Chem. Phys.* **120**, 7987 (2004).
45. R. Hellmann, E. Bich, E. Vogel, A. S. Dickinson, and V. Vesovic, *J. Chem. Phys.* **130**, 124309 (2009).
46. R. Hellmann, E. Bich, E. Vogel, and V. Vesovic, *Phys. Chem. Chem. Phys.* **13**, 13749 (2011).
47. M. Trautz and R. Heberling, *Ann. Phys.* **10**, 155 (1931).
48. G. A. Olchowy and J. V. Sengers, *Phys. Rev. Lett.* **61**, 15 (1988).
49. R. Mostert, H. R. van Den Berg, P. S. van der Gulik, and J. V. Sengers, *Physica A* **173**, 332 (1990).
50. P. T. Boggs, R. H. Byrd, J. H. Rogers, and R. B. Schnabel, *ODRPACK, Software for Orthogonal Distance Regression, NISTIR 4834, v2.013* (National Institute of Standards and Technology, Gaithersburg, MD, 1992).
51. G. A. Olchowy and J. V. Sengers, *Int. J. Thermophys.* **10**, 417 (1989).
52. R. A. Perkins, J. V. Sengers, I. M. Abdulagatov, and M. L. Huber, *Int. J. Thermophys.* **34**, 191 (2013).